# Computational experiments with inexact restoration techniques to solve topological optimization problems with unilateral boundary conditions

S. L. C. Castro [*] E. A. Fancello [†] A. Friedlander S. A. Santos [‡]

**Abstract**

The aim of this paper is to study the resolution of topological optimization in contact problems via an inexact restoration algorithm for solving bilevel programming problems. We present computational experiments for bi-dimensional frames. The problem is to minimize the strain energy subject to volume constraints and frictionless contact.

In structural optimization the free variables of an optimization problem are usually only the design variables. The displacement field is considered a function of the design variables, that are given implicitly through the equilibrium constraints. Many algorithms used to solve these problems compute at each iteration of the optimization process a solution of the equilibrium constraints and use the adjoint method to make the sensitivity analysis.

The approach presented here treats all the constraints and variables explicitly. We allow infeasibilities during the optimization process and work with all the variables as independent, so the sensibility analysis simplifies considerably. The algorithm consists of two phases, one related with feasibility and the other with optimality. We are free to choose any efficient algorithm for each of the phases. It is not necessary to use non-smooth algorithms.

**Key words:** Topological Optimization, Contact Problems, Bilevel Programming, Inexact-Restoration.

[*]Faculdades Integradas Metropolitanas de Campinas-METROCAMP, Campinas SP, Brazil.

[†]Department of Mechanical Engineering - GRANTE, Federal University of Santa Catarina, Florianópolis, SC,Brazil.

[‡]Department of Applied Mathematics, IMECC-UNICAMP, University of Campinas, Campinas SP, Brazil.

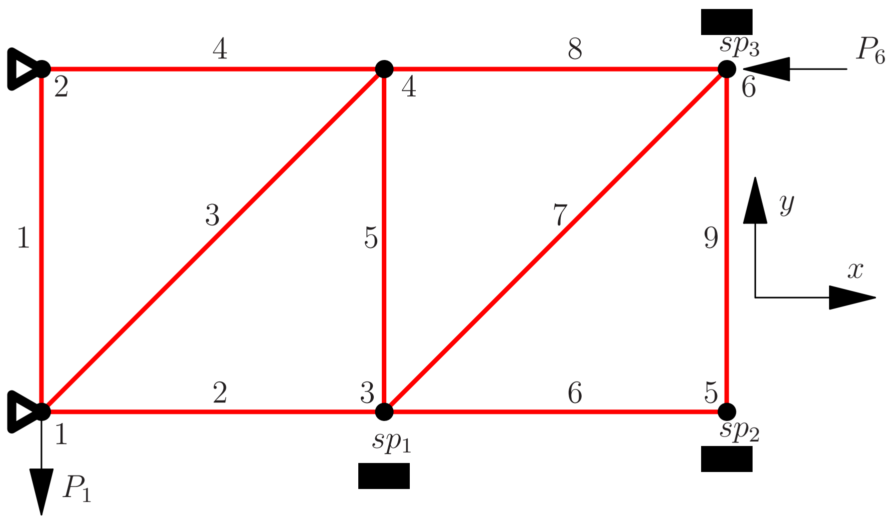


Figure 1: Configuration of the nine-truss frame.

# 1 A nine-truss frame system

We study the nine-truss frame system shown in figure 1. The length of each truss is denoted by $l_i$ and its cross section area by $A_i$, for $i = 1, \dots, 9$.

We assume that the displacements at nodes 1 and 2 are only vertical. Vertical and horizontal loads may be applied on the nodes and three rigid obstacles are at positions $sp_1$, $sp_2$, $sp_3$.

The structural optimization problem consists in finding the value of the cross section that maximizes the stiffness of the system under a volume (material) constraint. In the mathematical formulation of this problem the design variables are the cross section areas $A_i$ and the objective function to be minimized is the system's strain energy. The constraints represent the equilibrium of the system, that in this case is a frictionless contact problem, and the upper bound of the volume. It can be formulated as the following bilevel programming problem:

$$
\begin{array}{ll}
\underset{A,u}{\text{Minimize}} & W(A,u) \\
\text{subject to} & \left\{ \begin{array}{l} 0 \leq A_i \leq \overline{A} \\ V(A) - \overline{V} \leq 0 \\ \quad u = \underset{u}{\text{argmin}} \quad W_\alpha(A,u) - P^T u \\ \qquad\quad \text{s.t.} \qquad\quad u \in K \end{array} \right.
\end{array}
\tag{1}
$$

where $A \in I\!R^9$ is the vector of the cross section areas, $u \in I\!R^{12}$ is the vector of displacements and $V = \sum_{i=1}^{9} A_i l_i$ is the total volume of the bars effectively used at any frame configuration and $u \in I\!R^{12}$ is the vector containing the displacements of the six nodes of the structure. The displacement components at each node $k$ are such that

$$u_x^k = u_{2k-1} \quad u_y^k = u_{2k}.$$

Directions $x$ and $y$ are coincident with the directions of the global coordinate system (see Figure 1). The set of admissible displacements is given by $K = \{U \in I\!R^{12} \mid u_1 = 0,\ \ u_3 = 0,\ \ u_6 \geq sp_1,\ \ u_{10} \geq sp_2 \text{ and } u_{12} \leq sp_3\}$. The elastic strain energy stored in the frame is given by $W = \sum_{i=1}^{9} w_i$ where $w_i$ is the contribution of each truss of the frame:

$$w_i = \frac{A_i E}{2l_i}(\nu_1^i\ \nu_2^i\ \nu_3^i\ \nu_4^i) \begin{pmatrix} c^2 & cs & -c^2 & -cs \\ cs & s^2 & -cs & -s^2 \\ -c^2 & -cs & c^2 & cs \\ -cs & -s^2 & cs & s^2 \end{pmatrix} \begin{pmatrix} \nu_1^i \\ \nu_2^i \\ \nu_3^i \\ \nu_4^i \end{pmatrix}, i = 1, \ldots, 9.$$

In this last expression $(\nu_1^i\ \nu_2^i\ \nu_3^i\ \nu_4^i)$ are the displacements of the first and second nodes of the $i$-th truss, and $c = \cos\theta,\ \ s = \sin\theta$, where $\theta$ is the angle between the truss and the $x$ axes of the global coordinate system. We consider $(A, u) \in \Omega$ a compact set and $\overline{V}$ is the maximum volume allowed, and $P$ is the vector of loads. We also introduce a regularization in the lower level objective function adding a term involving the vertical displacement at node 2 as follows:

$$W_\alpha(A, u) = W(A, u) + \frac{1}{2}k(u_4)^2 \quad k \ll \frac{A_i E}{l_i}\ \forall\, i = 1, ..., 9$$

## 2 Inexact restoration technique for bilevel programming problems

The inexact-restoration algorithm introduced in [6] is an iterative method for solving nonlinear programming problems, that at each iteration determines using two phases, a new approximation of the solution. In the first phase, called restoration phase, it seeks for a more feasible point. In the second one, called the optimization phase it finds a point that sufficiently decreases the Lagrangian of the problem in an approximated tangent set. A merit function is used to measure the progress of the whole process.

An adaptation of the inexact-restoration approach for bilevel problems was proposed in [1] to deal with problems formulated as:

$$\begin{array}{ll} \underset{r,s}{\text{Minimize}} & F(r,s) \\ \text{s.t.} & \left\{ \begin{array}{l} s = \underset{s}{\text{argmin}} \quad f(r,s) \\ \qquad \text{s.t.} \quad \left\{ \begin{array}{l} h(r,s) = 0 \\ s \geq 0 \end{array} \right. \end{array} \right. \end{array} \tag{2}$$

where $r \in X$, $s \in Y$, $F, f : I\!R^{n_r+n_s} \to I\!R$ and $h : I\!R^{n_r+n_s} \to I\!R^m$ are continuous, and $\nabla F(r,s)$, $\nabla f(r,s)$ and $\nabla h(r,s)$, exist and are continuous.

The technique proposed proceeds at each iteration, as in the nonlinear programming case, in two different phases to improve respectively the feasibility and the optimality. The main advantage in this case is that the follower's problem, that characterizes the feasible set, can be solved, in the restoration phase, without reformulation.

In order to solve problem (2), some definitions and specifications on the original algorithm are necessary and, under some assumptions, it can be proved that the proposed algorithm is well defined an converge to feasible points satisfying the AGP optimality condition(see [2]).

Given an approximated solution $(A^k, u^k)$ of problem (1), the two phases of the algorithm proceed as follows to find a new approximation $(A^{k+1}, u^{k+1})$

**Restoration Phase:**

The problem we want to solve inexactly in this phase is,

$$\begin{array}{ll} \underset{u}{\text{Minimize}} & W_\alpha(A^k, u) - P^T u \\ \text{s.t.} & \left\{ \begin{array}{l} u_1 = 0 \\ u_3 = 0 \\ u_6 \geq sp_1 \\ u_{10} \geq sp_2 \\ u_{12} \leq sp_3. \end{array} \right. \end{array} \tag{3}$$

As the variables $u_1 = u_3 = 0$ are fixed, we substitute this values in the objective function and the problem can be written as:

$$\begin{array}{ll} \underset{u}{\text{Minimize}} & W_\alpha(A^k, u) - P^T u \\ \text{s.t.} & \left\{ \begin{array}{l} u_6 - y_1 = sp_1 \\ u_{10} - y_2 = sp_2 \\ u_{12} + y_3 = sp_3 \\ y_1 \geq 0, y_2 \geq 0, y_3 \geq 0 \end{array} \right. \end{array} \tag{4}$$

where $u = (u_2, u_4, u_5, \ldots, u_{12}) \in I\!R^{10}$, $P = (P_2, P_4, P_5, \ldots, P_{12}) \in I\!R^{10}$. We define $z = (y_1, y_2, y_3)^T$.

In the restoration phase we seek for a new approximation $(A^k, \bar{u}, \bar{z})$, solving inexactly the second level problem (equilibrium problem) parameterized by $A^k$. For this we use any convenient optimization algorithm. The KKT optimality conditions of this problem are used as a measure of feasibilty and furnishes a stopping criterium for the optimization algorithm used in this phase as follows:

$$|C(A^k, \bar{u}, \bar{z}, \bar{\mu})| \leq r|C(A^k, u^k, z^k, \mu^k)| \tag{5}$$

where $C(A, u, z, \mu)$ are the equalities of the KKT system associated to the equilibrium problem, and $\bar{\mu}$ is an estimative of the vector of Lagrange multipliers at $(A^k, \bar{u}, \bar{z})$.

$$C(A, u, z, \mu) = \begin{pmatrix} \nabla_u[W_\alpha(A, u)] - P + \mu_1 e_6 + \mu_2 e_{10} + \mu_3 e_{12} \\ -\mu_1 + \mu_4 \\ -\mu_2 + \mu_5 \\ \mu_3 + \mu_6 \\ u_6 - y_1 - sp_1 \\ u_{10} - y_2 - sp_2 \\ u_{12} + y_3 - sp_3 \\ \mu_4 y_1 \\ \mu_5 y_2 \\ \mu_6 y_3 \end{pmatrix}$$

with $\nabla_u[W_\alpha(A, u)],\ P,\ e_6,\ e_{10},\ e_{12} \in I\!R^{10}$, where each $e_i$ is the corresponding vector in the canonical basis of $I\!R^{10}$.

**Minimization phase**:

In this phase we find a new approximation $(\hat{A}, \hat{u}, \hat{z}, \hat{\mu}) \in \Pi_k$, such that:

$$L(\hat{A}, \hat{u}, \hat{z}, \hat{\mu}, \lambda^k) \ll L(A^k, \bar{u}, \bar{Y}, \bar{\mu}, \lambda^k) \tag{6}$$

and

$$\|(\hat{A}, \hat{u}, \hat{z}, \hat{\mu}) - (A^k, \bar{u}, \bar{z}, \bar{\mu})\| \leq \delta_k \tag{7}$$

where

$$\Pi_k = \{v \in \Lambda \mid C'(A^k, \bar{u}, \bar{z}, \bar{\mu})(s - A^k, \bar{u}, \bar{z}, \bar{\mu}) = 0\}$$

is the approximate tangent set to the feasible region and

$$L(A, u, z, \mu, \lambda) = W(A, u) + \langle C(A, u, z, \mu), \lambda \rangle$$

is the Lagrangian function and $\ll$ means a sufficient decrease.

We obtain the new approximation $(\hat{A}, \hat{u}, \hat{z}, \hat{\mu})$ solving the following optimization problem:

$$
\begin{array}{ll}
\underset{A,u,z,\mu}{\text{Minimize}} & L(A,u,z,\mu,\lambda) = W(A,U) + \langle C(A,u,z,\mu), \lambda \rangle \\
\text{s.t.} & \left\{ \begin{array}{l} 0 \leq A_i \leq \overline{A} \\ V(A) - \overline{V} \leq 0 \\ C'(A^k, \bar{u}, \bar{Y}, \bar{\mu})((A,u,z,\mu) - (A^k, \bar{u}, \bar{z}, \bar{\mu})) = 0 \\ y_1 \geq 0, y_2 \geq 0, y_3 \geq 0 \\ \mu_4 \geq 0, \mu_5 \geq 0, \mu_6 \geq 0 \end{array} \right.
\end{array}
\quad (8)
$$

A merit function of the sharp Lagrangian type is used to decide if this point is accepted.

# 3 Computational experiments

To solve problem (1), we considered the following data:

- Upper bound for cross section areas: $A_i = 4\ mm^2$ $(i = 1, ..9)$;
- $l_i = 200\ mm$ for horizontal bars $(i = 2, 4, 6, 8)$ and vertical bars $(i = 1, 5, 9)$ e $l_i = 200\sqrt{2}\ mm$ for the diagonal bars $(i = 3, 7)$;
- $E = 2 \times 10^5\ N/mm^2$;
- Upper bound $\overline{V} = 25\%$ of the maximum volume i.e., considering all the bars with their maximum value of cross section area.

In table 1 we summarize the choices done in five cases. Our initial point was $A_i = 4\ mm^2$, $i = 1, \ldots, 9$ e $u_j = 0\ mm$, $j = 1, \ldots, 12$. All the other variables (slacks and multipliers) were initialized at zero. In the restoration and minimization phases, we used the package MINOS ([7]) in order to solve the minimization problems. To estimate the vector of Lagrange multipliers $\mu$ of the follower's problem we used the least square approach and to update $\lambda$ we used the estimations given by the optimization package MINOS, used in the minimization phase.

## 3.1 Case 1

The results are shown in tables 2-5. The optimal structure is in figure 2 (left.). Execution time was 99.4 seconds. The pattern of the displacements is presented out of scale in figure 2 (right). In this way we can see optimal displacements corresponding to the optimal frame. We observe that the maximum volume is achieved and the feasibility error is of the order of $2 \times 10^{-12}$.

Table 1: Experiments with the nine-truss frame.

| Case | Position of obstacles (mm) | Loads (N) |
|---|---|---|
| 1 | $sp_1 = 0, sp_2 = 0, sp_3 = 0$ | $P_1 = -100$ $P_6 = 0$ |
| 2 | $sp_1 = -1, sp_2 = 0, sp_3 = 0$ | $P_1 = -100$ $P_6 = 0$ |
| 3 | $sp_1 = -1, sp_2 = 0, sp_3 = 1$ | $P_1 = +100$ $P_6 = 0$ |
| 4 | $sp_1 = 0, sp_2 = 0, sp_3 = 0$ | $P_1 = -100$ $P_6 = -100$ |
| 5 | $sp_1 = -1, sp_2 = 0, sp_3 = 0$ | $P_1 = -100$ $P_6 = -200$ |

Table 2: First-level objective function - Case 1

| Iteration | Strain energy | Feasibility error |
|---|---|---|
| Initial (0) | 0.00 | 100.00 |
| Final (20) | 6.39 | 2.34 $\times 10^{-12}$ |

Table 3: Cross section areas - Case 1

| Bar $i$ | $A_i$ |
|---|---|
| 1 | 0.00 |
| 2 | 1.22 $\times 10^{-7}$ |
| 3 | 4.00 |
| 4 | 3.50 |
| 5 | 3.50 |
| 6 | 0.00 |
| 7 | 1.57 $\times 10^{-7}$ |
| 8 | 9.89 $\times 10^{-8}$ |
| 9 | 0.00 |

Table 4: Nodal displacements - Case 1

| Node | $u_x = u_{2i-1}$ | $u_y = u_{2i}$ |
|---|---|---|
| 1 | 0.00 | -1.28 $\times 10^{-1}$ |
| 2 | 0.00 | -1.71 $\times 10^{-1}$ |
| 3 | -6.44 $\times 10^{-3}$ | 0.00 |
| 4 | -2.86 $\times 10^{-2}$ | -2.86 $\times 10^{-2}$ |
| 5 | -9.24 $\times 10^{-3}$ | 1.54 $\times 10^{-3}$ |
| 6 | -2.06 $\times 10^{-2}$ | 0.00 |

Table 5: Contact forces - Case 1.

| Node | Force |
|---|---|
| 3 | 100.00 |
| 5 | 0.00 |
| 6 | $7.86 \times 10^{-7}$ |

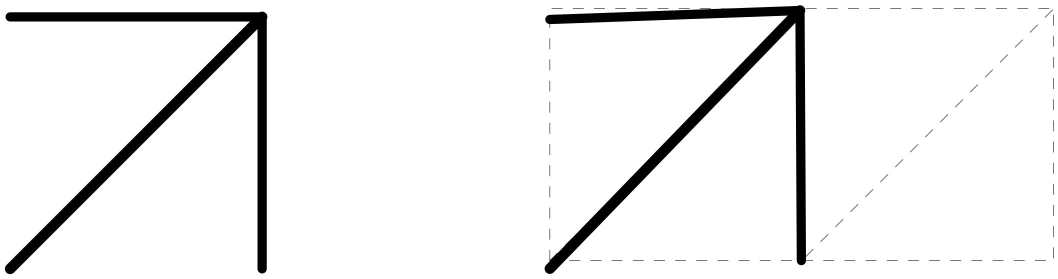

Figure 2: Optimal configuration (left) and displacements pattern (right) for case 1.

### 3.2 Case 2

The results are shown in tables 6-9. The optimal structure is in figure 3 (left.). Execution time was 48.89 seconds. The pattern of the displacements is presented out of scale in figure 3 (right). The maximum volume is achieved and the feasibility error is of the order of $1 \times 10^{-6}$.

### 3.3 Case 3

The results are shown in tables 10-13. The optimal structure is in figure 4 (left.). Execution time was 100.04 seconds. The pattern of the displacements is presented out of scale in figure 4 (right). The maximum volume is achieved and the feasibility error is of the order of $8 \times 10^{-6}$.

Table 6: First-level objective function - Case 2

| Iteration | Strain energy | Feasibility error |
|---|---|---|
| Initial (0) | 0.000 | 100.01 |
| Final (8) | 39.50 | $1.15 \times 10^{-6}$ |

Table 7: Cross section areas - Case 2

| Bar $i$ | $A_i$ |
|---|---|
| 1 | 0.00 |
| 2 | 1.27 |
| 3 | 1.79 |
| 4 | 2.53 |
| 5 | 1.27 |
| 6 | 0.00 |
| 7 | 1.79 |
| 8 | 1.27 |
| 9 | 1.27 |

Table 8: Nodal displacements - Case 2

| Node | $u_x = u_{2i-1}$ | $u_y = u_{2i}$ |
|---|---|---|
| 1 | 0.00 | -7.90 $\times 10^{-1}$ |
| 2 | 0.00 | -7.81 $\times 10^{-1}$ |
| 3 | 7.9 $\times 10^{-2}$ | -4.74 $\times 10^{-1}$ |
| 4 | -7.9 $\times 10^{-2}$ | -5.53 $\times 10^{-1}$ |
| 5 | 8.98 $\times 10^{-2}$ | 0.00 |
| 6 | -1.58 $\times 10^{-1}$ | -7.90 $\times 10^{-2}$ |

Table 9: Contact forces - Case 2.

| Node | Force |
|---|---|
| 3 | 0.00 |
| 5 | 100.00 |
| 6 | 0.00 |

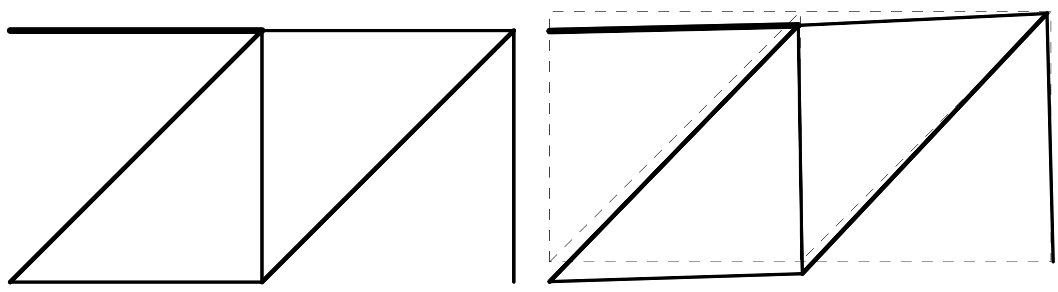

Figure 3: Optimal Configuration (left) and displacements pattern (right) for case 2.

Table 10: First-level objective function - Case 3

| Iteration | Strain energy | Feasibility error |
|---|---|---|
| Initial (0) | 0.000 | 100.01 |
| Final (18) | 32.00 | $8.84 \times 10^{-6}$ |

Table 11: Cross section areas - Case 3

| Bar $i$ | $A_i$ |
|---|---|
| 1 | 0.00 |
| 2 | 1.41 |
| 3 | 1.99 |
| 4 | 2.81 |
| 5 | 1.41 |
| 6 | 0.00 |
| 7 | 1.99 |
| 8 | 1.41 |
| 9 | 0.00 |

Table 12: Nodal displacements - Case 3

| Node | $u_x = u_{2i-1}$ | $u_y = u_{2i}$ |
|---|---|---|
| 1 | 0.00 | 1.64 |
| 2 | 0.00 | 1.64 |
| 3 | $-7.12 \times 10^{-2}$ | 1.36 |
| 4 | $7.12 \times 10^{-2}$ | 1.43 |
| 5 | $-7.00 \times 10^{-2}$ | 1.00 |
| 6 | $1.42 \times 10^{-1}$ | 1.00 |

Table 13: Contact forces - Case 3.

| Node | Force |
|---|---|
| 3 | 0.00 |
| 5 | 0.00 |
| 6 | 100.00 |

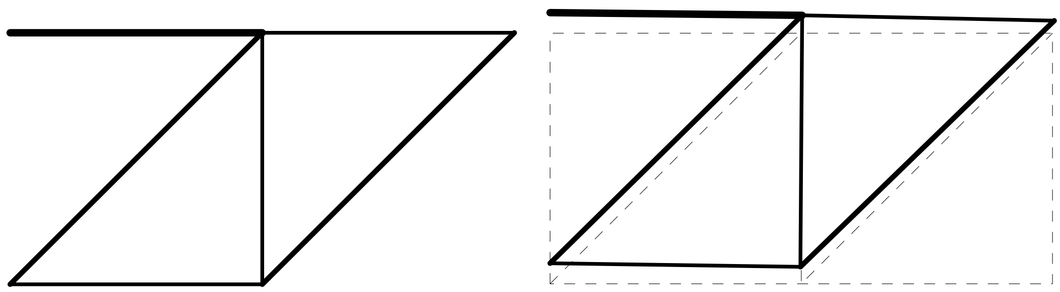

Figure 4: Optimal configuration (left) and displacements pattern (right) for case 3.

Table 14: First-level objective function - Case 4

| Iteration | Strain energy | Feasibility error |
|---|---|---|
| Initial (0) | 0.00 | 141.42 |
| Final (11) | 14.24 | $5.38 \times 10^{-11}$ |

## 3.4 Case 4

The results are shown in tables 14-17. The optimal structure is in figure 5 (left.). Execution time was 59.08 seconds. The pattern of the displacements is presented out of scale in figure 5 (right). The maximum volume is achieved and the feasibility error is of the order of $5 \times 10^{-11}$.

Table 15: Cross section areas - Case 4

| Bar $i$ | $A_i$ |
|---|---|
| 1 | 0.00 |
| 2 | 0.00 |
| 3 | 3.06 |
| 4 | 4.00 |
| 5 | 2.16 |
| 6 | 0.00 |
| 7 | $2.50 \times 10^{-6}$ |
| 8 | 2.16 |
| 9 | 0.00 |

Table 16: Nodal displacements - Case 4

| Node | $u_x = u_{2i-1}$ | $u_y = u_{2i}$ |
|---|---|---|
| 1 | 0.00 | -1.89 $\times 10^{-1}$ |
| 2 | 0.00 | -2.07 $\times 10^{-1}$ |
| 3 | -9.62 $\times 10^{-2}$ | 0.00 |
| 4 | -5.00 $\times 10^{-2}$ | -4.62 $\times 10^{-2}$ |
| 5 | -1.97 $\times 10^{-2}$ | 1.54 $\times 10^{-3}$ |
| 6 | -9.62 $\times 10^{-2}$ | 0.00 |

Table 17: Contact forces - Case 4.

| Node | Force |
|---|---|
| 3 | 100.00 |
| 5 | 0.00 |
| 6 | 3.00 $\times 10^{-12}$ |

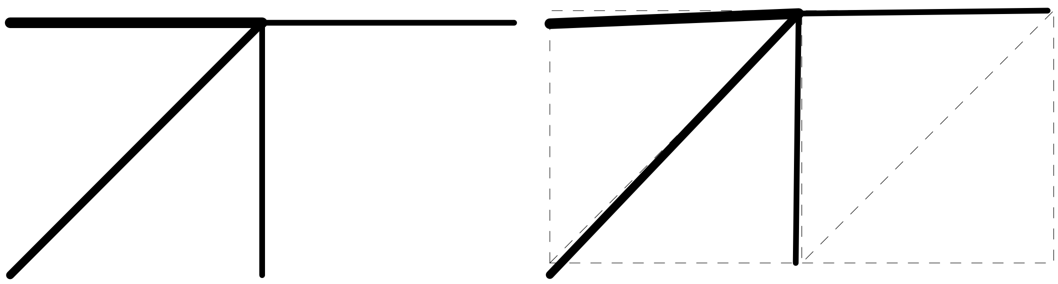

Figure 5: Optimal configuration (left) and displacements pattern (right) for case 4.

Table 18: First-level objective function - Case 5

| Iteration | Strain energy | Feasibility error |
|---|---|---|
| Initial (0) | 0.00 | 223.61 |
| Final (8) | 77.43 | $4.80 \times 10^{-5}$ |

Table 19: Cross section areas - Case 5

| Bar $i$ | $A_i$ |
|---|---|
| 1 | 0.00 |
| 2 | $9.04 \times 10^{-1}$ |
| 3 | 1.28 |
| 4 | 3.62 |
| 5 | $9.04 \times 10^{-1}$ |
| 6 | 0.00 |
| 7 | 1.28 |
| 8 | 2.71 |
| 9 | $9.04 \times 10^{-1}$ |

### 3.5 Case 5

The results are shown in tables 18-21. The optimal structure is in figure 6 (left.). Execution time was 52.94 seconds. The pattern of the displacements is presented out of scale in figure 6 (right). The maximum volume is achieved and the feasibility error is of the order of $5 \times 10^{-5}$.

# 4 Conclusions and the future work

In this work we presented a method to solve a frame optimization problem with frictionless contact formulated as a bilevel problem. We validated our results solving simultaneously

Table 20: Nodal displacements - Case 5

| Node | $u_x = u_{2i-1}$ | $u_y = u_{2i}$ |
|---|---|---|
| 1 | 0.00 | -1.11 |
| 2 | 0.00 | $-9.69 \times 10^{-1}$ |
| 3 | $1.12 \times 10^{-1}$ | $-6.64 \times 10^{-1}$ |
| 4 | $-1.11 \times 10^{-1}$ | $-7.74 \times 10^{-1}$ |
| 5 | $6.55 \times 10^{-2}$ | 0.00 |
| 6 | $-2.21 \times 10^{-1}$ | $-1.11 \times 10^{-1}$ |

Table 21: Contact forces - Case 5.

| Node | Force |
|---|---|
| 3 | 0.00 |
| 5 | 100.00 |
| 6 | 0.00 |

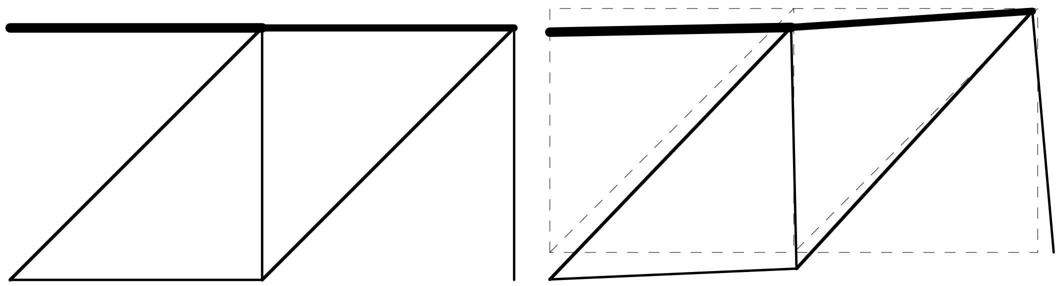

Figure 6: Optimal configuration (left) and displacements pattern (right) for case 5.

the problems with an algorithm described in [4, 5]

The inexact-restoration approach for bilevel problems has the advantage that the derivative and the Jacobian matrix of the cost function is easier to compute than in the classical formulation, since the variables (design variable and the solution of the equilibrium problem) are treated as independent. Also, it allows direct solving of the follower's problem that describes the equilibrium of the system. Moreover, the precision of the solution of the equilibrium problem is controlled at each iteration and it permits its inexact solving when we are far from the solution.

This approach also permits to deal naturally with nonlinear path-independent materials. The algorithm has shown to be reliable and the experimental results encourage us to improve implementation details. For solving larger problems we intend to exploit the characteristics of the topological optimization bilevel problem, that is a problem with a lot of structure.

# References

[1] Castro, S. L. C., *Técnica de Restauração Inexata aplicada à resolução de Problemas de Programação Matemática em Dois Níveis*, Ph.D. Dissertation, Universidade Estadual de Campinas, UNICAMP, Campinas, Brasil, 2004.

[2] Castro, S. L. C. and Friedlander, A., 2004. *Algoritmo de Restauração Inexata aplicado à resolução de problemas de Programação Matemática em Dois Níveis.* Technical Report. *www.ime.unicamp.br/ ˜ friedlan.*

[3] Fancello, E. A., *Topology optimization for minimum mass design considering local failure constraints and contact boundary conditions*, Structural and Multidisciplinary Optimization, 32 (3), 229–240, 2006.

[4] Fancello, E. A. and Feijóo, R. A., *Shape optimization in frictionless contact problems*, International Journal for Numerical Methods in Engineering, 37(38), 2311 – 2335, 1994.

[5] Fancello, E. A. and Pereira, J. T., *Structural topology optimization considering material failure constraints and multiple load conditions*, Latin American Journal Of Solids And Structures, 1(1), 3–25, 2003.

[6] Martínez, J. M., *Inexact-Restoration Method with Lagrangian Tangent Decrease and New Merit Function for Nonlinear Programming*, JOTA, 111(1), 39–58, 2001.

[7] Murtagh, B. A. & Saunders, M. A., *User's Guide*, Technical Report SOL 83-20, Stanford University. 1995

[8] J.S. Przemieniecki, *Theory of Matrix Structural Analysis*, Dover, 1985.